

Comparative Analysis on De-Noising of MRI Uterus Image for Identification of Endometrial Carcinoma

S Brindha ^{1*} , Judith Justin ²

¹ Research Scholar, Department of Biomedical Instrumentation Engineering, Avinashilingam Institute for Home Science and Higher Education for Women, Coimbatore, India

² Department of Biomedical Instrumentation Engineering, Avinashilingam Institute for Home Science and Higher Education for Women, Coimbatore, India

*Corresponding Author: S Brindha
Email: brindha.bliss@gmail.com

Received: 29 June 2022 / Accepted: 27 August 2022

Abstract

Purpose: The anatomical and physiological processes of the human body are pictured in radiology using different modalities. Magnetic Resonance Imaging (MRI) supports capturing the images of organs using magnetic field gradients. The quality of MR images is generally affected by various noises such as Gaussian, speckle, salt and pepper, Rayleigh, Rican etc. Removal of these noises from the MR images is essential for further diagnostic procedures.

Materials and Methods: In this article, Gaussian noise, speckle noise, and salt and pepper noise are added to the MR uterus image for which different filters are applied to remove the noise for precise identification of endometrial carcinoma.

Results: The different filters incorporated for the additive noise removal process are the bilateral filter, Non-Local Means (NLM) filter, anisotropic diffusion filter, and Convolution Neural Network (CNN). The efficiency of the filter is calculated by evaluating the response of the filter by gradually increasing the noise intensity of the MR images.

Conclusion: Further, peak Signal-to-Noise Ratio (SNR), structural similarity index measure, image quality index and computational cost parameters are computed and analyzed.

Keywords: Endometrial Carcinoma; Anisotropic Diffusion; Bilateral Filter; Non-Local Means Filter.

1. Introduction

The uncontrolled growth of the healthy cells forming a mass is termed a tumor. A tumor can be cancerous or benign. A cancerous tumor grows and spreads to other parts of the body, whereas a benign tumor grows but generally does not spread to other tissues. The most common cancer, which occurs in a woman's reproductive system, is uterine cancer. Uterine cancer can be categorized as adenocarcinoma and uterine sarcoma. Among the two major types of uterine cancer, adenocarcinoma that occurs in the endometrial layer is identified to be the most frequently occurring type of cancer. Various modalities such as ultrasound, computed tomography, and Magnetic Resonance Imaging (MRI) are considered for detecting and identifying the grade of tumors and the extent to which the cancerous cells have developed [1]. Images obtained from these modalities are processed to identify the nature of the uncontrolled growth of the human cell.

The Signal-to-Noise Ratio (SNR) is vital in generating quality information from the images obtained using different modalities. Various mathematical models support processing medical images based on different applications. The removal of noise and the signal estimation using different mathematical models are conventionally available [2].

In Magnetic Resonance (MR) imaging, de-noising and extracting the required information is a vital process for further proceedings. MR imaging is a non-invasive method that uses radiofrequency pulses to diagnose the nature of tissues in the human body's internal organs.

The SNR and high resolution of images are inversely proportional to each other. It is essential to maintain a balance between the resolution and SNR of MR images. The image obtained using the MRI modality from a human anatomical structure consists of both the information pixels and the noise pixels. Better resolution with high SNR is essential for extracting the required information by eliminating the noise pixels. Filtering with better edge-preserving ability is an essential process to denoise the images [3].

1.1. Related Works

Akdemir Akar proposed an edge-preserving method using a bilateral filter for denoising Rician noise from

MR images. Optimizing the bilateral filter parameters was done by the use of a genetic algorithm. These parameters are further investigated with both simulated and clinical MR images and validated using quantitative metrics. The performance of de-noising using a bilateral filter depends majorly on the selection of optimal parameters [1]. Liu bin *et al.* proposed an appropriate fuzzy cluster criterion in combination with a Non-Local Means (NLM) filter. The evaluation made for denoising synthetic brain MR images shows that the noise was suppressed without any changes in the details of the image. The computation time was also reduced to a greater extent [4].

Liu Chang *et al.* proposed a two-stage denoising algorithm based on a three-dimensional optimized block-wise version of non-local means and multidimensional Principle Component Analysis (PCA). The complete block representation of non-local means three-dimensional was considered to restore the noisy slice from nearby slices and a post-processing step was performed for noise removal. This structural information of three-dimensional MRI was also preserved. A better result was achieved by comparing the evaluation criteria with three-dimensional anisotropic diffusion filtering, non-local means three-dimensional [5].

Geng Cheng *et al.* proposed an algorithm to overcome the aggravated partial volume effects and blurred structures by matching the neighborhood non-flat domains using improved NLM. The noise along the x-spatial domain and q-spatial domain are also removed and q-space sampling domains were encoded using a graphical method. The resultant was utilized to locate the recurrent information. Finally, the denoising was performed by using the NLM framework. This method proves to be more effective in locating the recurrent information in white matter structure with various orientations [6].

Yousefi Moteghaed *et al.* focus on sequence filters selected by using a hybrid genetic algorithm and Particle Swarm Optimization (PSO) implemented on medical images with noises. Statistical analysis based on peak SNR, Structural Similarity Index Measure (SSIM), and Root Mean Square Error (RMSE) were performed and the result shows an increase in the visual quality of the image [7].

Table 1 shows the performance of various filters in terms of Peak Signal-to-Noise Ratio (PSNR) and Structural Similarity Index Measure (SSIM).

Table 1. Performance of various filters in terms of PSNR and SSIM

Study	Filter	Noise Density (%)	PSNR in dB	SSIM
Saime Akdemir Akar, 2016 [1]	Bilateral Filter	Rician Noise 10% - 30%	20.4688	0.6499
B. Liu, 2015 [4]	Non Local Means		19.0993	0.4018
	Wavelet Method	Rician Noise 1% - 15%	19.2956	0.3772
	NLM with Fuzzy Clustering		25.8403	0.4020
Liu Chang, 2015 [5]	Anisotropic Diffusion Filter		25.3515	0.7604
	NLM3D	Rician Noise 3%-5%	34.5518	0.9472
	NLM-MPCA		35.5598	0.9555
Geng Chen, 2020 [6]	Adaptive NLM		14.52	
	NL spatial & angular matching	Gaussian Noise 1% -9%	22.90	NA
	x - q space non-local means		22.74	
	Graph Framelet Matching		23.18	
N.Yousefi Moteghaed, 2020 [7]	Genetic Algorithm	Noise Model 1 (1-5%) { Gaussian Noise, Salt & Pepper Noise, Speckle Noise }	57.01	0.9982
	Particle Swarm Optimization		63.72	0.9991
	GA-PSO		63.50	0.9997
	Genetic Algorithm	Noise Model 2 (6-10%) { Gaussian Noise, Salt & Pepper Noise, Speckle Noise }	56.73	0.9990
	Particle Swarm Optimization		60.75	0.9991
	GA-PSO		63.50	0.9992
R.Kala, 2019 [8]	Median Filter		18.77	0.25
	NLM Filter		14.03	-
	Adaptive Filter		17.90	-
	Bilateral Filter	Rician Noise 1% - 10%	64.67	0.98
	Wiener Filter		18.73	0.16
	Fuzzy-NLM		18.27	0.21
	Adaptive Fuzzy Hexagonal BF		66.66	0.99
M.H.O.Rashid, 2018 [9]	Median Filter		73.1668	
	Wiener Filter	Gaussian Noise	72.4354	NA
	Anisotropic Filter		73.9025	
	Median Filter		74.1484	
	Wiener Filter	Salt & Pepper Noise	72.4451	NA
	Anisotropic Filter		75.2181	
	Median Filter		80.8864	
	Wiener Filter	Speckle Noise	71.6502	NA
	Anisotropic Filter		77.9235	

2. Materials and Methods

In this article, the process involved in denoising the MR image of the uterus for endometrial carcinoma identification is elaborated. The system specification also decides the time complexity of the execution of the process. The processor used is Intel Core i3 Processor, 4GB RAM in a platform using MATLAB R2019a (64bit).

Figure 1 shows the flow chart of the process involved in denoising the MR image. A uterus image using the MRI modality is considered for identifying the cancerous cell in the endometrial layer. This image with endometrial carcinoma must be processed to observe the response to adding different noise pixels. The required information has to be segregated from the additive noise by the application of different filters accordingly. Among the various types of noises, speckle, Gaussian noise, and salt and pepper noise are considered for the denoising procedure. These noises are added gradually to the image to verify the performances of different filters applied. This process is inculcated based on the type and intensity of the noise applied. The responses of the filter are observed based on the variation in the additive noises. Bilateral filters, anisotropic diffusion, and NLM filters are used in this research to denoise the MR image. Different parameters such as PSNR, SSIM, Image Quality Index (IQI), and Time Complexity (TC) are computed, and the results are compared.

Bilateral Filter: It is one of the conventional filters used for image denoising. This filter is generally referred to as an edge-preserving filter and supports the noise reduction process. It also acts as a smoothing filter for images and is non-linear. Based on Gaussian distribution, the intensity of each pixel is replaced with a weighted

average of the intensity values of nearby pixels. The weight does not limit to the Euclidean distance of the pixels but also extends to radiometric differences such as color intensity, range difference, and depth distance. It supports preserving the sharp edges. Denoising the intensity of a pixel is achieved by calculating the weights and by normalizing them [1].

Non-Local Means (NLM) filter: It supports image denoising by considering the mean of all pixels in an image. The values are weighted by comparing the similarities of the pixels to the target pixel. The value obtained after the filtering process is good with the reduced informational loss [8].

Anisotropic Diffusion filtering: It aims to denoise the image without any loss of essential details. The edges, lines, and other details required for interpreting the image are well preserved by this filter. Anisotropic diffusion is similar to the scale-space process, where more blurred images generate a parameterized family based on the diffusion process [9].

CNN Filtering: CNN-based MRI denoising was performed using CNN-Denoising MRI model for reducing Gaussian noise, speckle noise, and salt and pepper noise. The CNN-model consists of multiple convolutions that support differentiating the noise pixels from the various features of the MRI image. Various subsections are provided for denoising using the CNN-Denoising MRI model [10].

Performance Metrics.PSNR: It is a ratio between the power of the signal and the power of corrupting noise. PSNR is described using mean square error. It also supports measuring the quality of information present in the image. Quality of the reconstructed image is

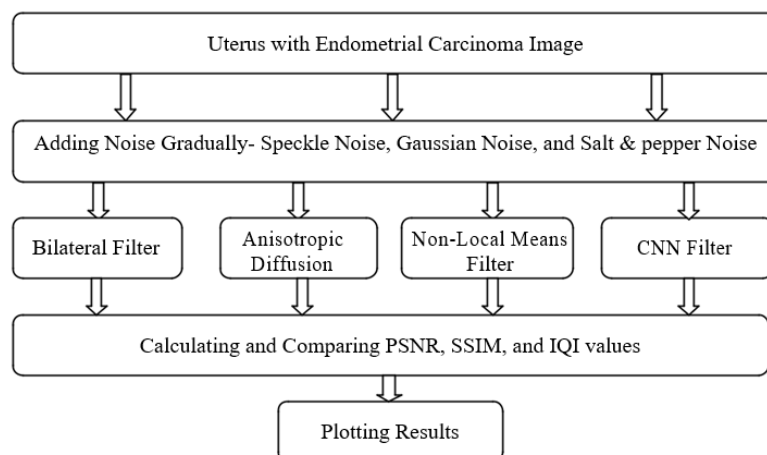


Figure 1. Flow chart of the proposed system

proportional to the value of PSNR, which means that the higher the PSNR, the better the quality of images [1].

The MSE is calculated, and the value obtained is used in computing the PSNR value. The following equation is used for MSE calculation.

$$MSE = \frac{\sum_{M,N}[I_1(m,n) - I_2(m,n)]^2}{M * N} \quad (1)$$

In Equation 1, the rows and columns of the input images are denoted using the variables M and N. The PSNR is computed using Equation 2.

$$PSNR = 10 \log_{10} \left(\frac{R^2}{MSE} \right) \quad (2)$$

In Equation 2, R - maximum fluctuation in the input image data type.

If the input image has a double-precision floating-point data type, then R is 1. If it has an 8-bit unsigned integer data type, R is 255.

Structural similarity index measure: It is the pixel, while having a strong interdependency during spatial closeness, that describes the structural information. It carries the required information regarding the structure of the object during the dependencies (Equation 3) [1].

$$SSIM = \frac{(2\mu_X\mu_{\hat{X}} + t_1)(2\sigma_{X\hat{X}} + t_2)}{(\mu_X^2 + \mu_{\hat{X}}^2 + t_2)(\sigma_X^2 + \sigma_{\hat{X}}^2 + t_2)} \quad (3)$$

Where μ_X and $\mu_{\hat{X}}$ are means of noisy-free image and denoised image; t_1 and t_2 are constants; σ_X^2 and $\sigma_{\hat{X}}^2$ represent the variances; $\sigma_{X\hat{X}}$ shows the covariance between X and \hat{X} .

Image quality index: Subjective and objective methods are used to assess image quality. The attribute or set of images assessed by a human's viewing perception is a

subjective method. In contrast, the perceptual image quality computed by a particular method is objective [11].

Time Complexity: The time taken to execute an algorithm as a function of the length of the input is considered as time complexity. It also supports measuring the time taken to execute each code in an algorithm. The time complexity also varies based on the specification of the hardware used [11].

The source images for the computation process were availed from the National Cancer Institute's Clinical Proteomic Tumor Analysis Consortium Uterine Corpus. Endometrial Carcinoma (CPTAC-UCEC) cohort (<https://wiki.cancerimagingarchive.net/display/Public/CPTAC-UCEC>).

De-noising the image obtained from various modalities is considered to be an unavoidable step in extracting the textural feature. In this module of the de-noising procedure, 699 images were considered with various angles of view, such as axial, sagittal, and transverse. From these images, the required quantity of images with certain views has been considered for the additive noise process. This was performed to identify the efficiency of various filters in removing different noises that commonly occur in the MR Imaging modality. Of 699 images total, 40 images for each filter were taken for the preprocessing procedure.

3. Results

Figure 2 shows Gaussian, Speckle, and Salt and Pepper noise added with the variance of 0.50 to the original image obtained using MR imaging modality. Figure 3 shows the filtered output images obtained using a bilateral filter, NLM filter, anisotropic diffusion filter, and CNN filter. These results were obtained by filtering the noisy images shown in Figure 2. From the analysis taken, it is observed that each filter outperforms in different performance

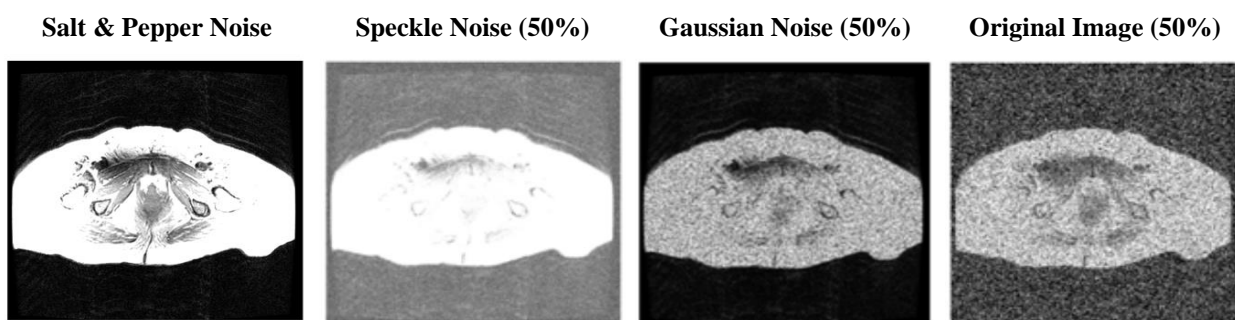


Figure 2. Additive noise images a) Original image b) Inclusion of 50% Gaussian noise c) Inclusion of 50% Speckle noise d) Inclusion of 50% Salt & Pepper noise

metrics of PSNR, SSIM, IQI, and time complexity. Tables 2, 3 and 4 show the performance matrices of

PSNR, SSIM, and, IQI for different filters with various percentage of additive noises.

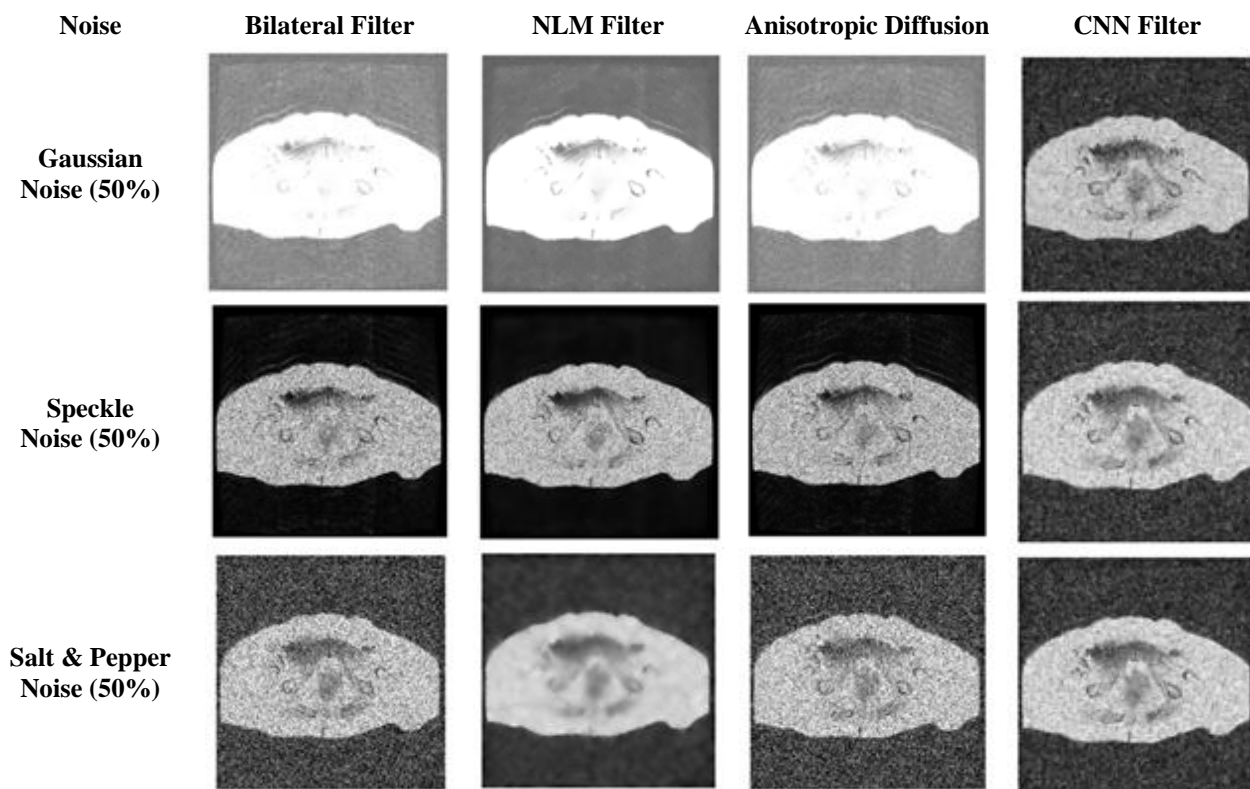


Figure 3. Filtered output images of Bilateral filter, NLM filter, Anisotropic Diffusion filter and CNN filter

Table 2. PSNR Calculation of three filters with three different noises in various ranges

Noise/PSNR	10	20	30	40	50	60	70	80	90
Gaussian									
Bilateral	24.9185	24.5281	24.0339	23.4766	22.8773	22.2507	21.6619	21.002	20.3886
NLM	27.2891	26.8705	26.2534	25.4483	24.6664	23.867	23.0515	22.2355	21.485
Anisotropic	22.6987	22.4462	22.0914	21.7196	21.3052	20.87	20.3876	19.8969	19.3967
CNN	28.00792	25.37029	23.7165	22.56803	21.63438	20.81521	20.18335	19.64068	19.0638
Speckle									
Bilateral	29.4036	25.9148	23.6633	22.1182	20.9683	20.0823	19.2749	18.6635	18.1009
NLM	27.5208	24.6336	22.9353	21.7788	20.7972	20.08	19.4454	18.8727	18.3654
Anisotropic	27.8181	24.3754	22.4807	21.2595	20.295	19.4706	18.8188	18.2305	17.6929
CNN	30.78756	28.10417	26.45428	25.33643	24.46813	23.71414	23.06931	22.53111	22.11742
Salt & Pepper									
Bilateral	23.0098	20.3768	18.5766	17.4622	16.437	15.6218	15.0152	14.455	13.9103
NLM	23.5717	20.1578	18.5197	17.381	16.9965	17.2069	17.6841	18.2954	18.8091
Anisotropic	23.5063	20.4942	18.584	17.5234	16.5592	15.7485	14.9784	14.3701	13.9264
CNN	24.41903	22.04745	20.81045	20.37298	19.94742	19.78272	19.59717	19.5538	19.39148

Table 3. SSIM Calculation of three filters with three different noises in various ranges

Noise/SSIM	10	20	30	40	50	60	70	80	90
Gaussian									
Bilateral	0.47776	0.47401	0.47153	0.47051	0.46787	0.46638	0.46468	0.46107	0.45756
NLM	0.65714	0.64667	0.63659	0.62298	0.60917	0.59593	0.58371	0.57035	0.55767
Anisotropic	0.34736	0.34842	0.34998	0.35309	0.35538	0.3625	0.36764	0.36965	0.37652
CNN	0.678797	0.615472	0.575854	0.543746	0.514943	0.493974	0.474628	0.45882	0.441961
Speckle									
Bilateral	0.82855	0.73216	0.68476	0.65969	0.6433	0.63007	0.62067	0.61327	0.60647
NLM	0.71109	0.62021	0.5744	0.54677	0.52575	0.51182	0.50013	0.49103	0.4824
Anisotropic	0.78291	0.71757	0.68801	0.66983	0.65649	0.64445	0.63512	0.62639	0.61704
CNN	0.946213	0.917357	0.895246	0.875936	0.859708	0.8459	0.834273	0.823331	0.81232
Salt & Pepper									
Bilateral	0.72773	0.59321	0.47662	0.39604	0.32972	0.27291	0.23814	0.20545	0.17911
NLM	0.74532	0.53448	0.42404	0.34399	0.30157	0.28729	0.28869	0.29507	0.30192
Anisotropic	0.77625	0.62076	0.49394	0.4205	0.35109	0.29448	0.24525	0.21118	0.18393
CNN	0.766881	0.615566	0.500767	0.435333	0.384752	0.354124	0.32819	0.311978	0.302409

Table 4. IQI Calculation of three filters with three different noises in various ranges

Noise/IQI	10	20	30	40	50	60	70	80	90
Gaussian									
Bilateral	0.29983	0.29458	0.28666	0.28073	0.27418	0.26744	0.26215	0.25496	0.24793
NLM	0.27395	0.27375	0.27979	0.27602	0.26975	0.26685	0.26731	0.27438	0.27229
Anisotropic	0.25038	0.248	0.2445	0.23985	0.23525	0.23212	0.2285	0.22284	0.22022
CNN	0.329059	0.284336	0.258389	0.235647	0.22145	0.21049	0.19777	0.190149	0.183557
Speckle									
Bilateral	0.63637	0.60988	0.59113	0.57815	0.56825	0.55751	0.55082	0.544	0.53785
NLM	0.4459	0.35057	0.30401	0.27261	0.25193	0.23704	0.22369	0.21397	0.20483
Anisotropic	0.6874	0.6594	0.64157	0.62809	0.61689	0.60618	0.59664	0.58736	0.57735
CNN	0.695707	0.664618	0.63548	0.610668	0.587794	0.568959	0.552319	0.53682	0.522237
Salt & Pepper									
Bilateral	0.64893	0.51953	0.41082	0.33745	0.27729	0.22846	0.19957	0.17362	0.15209
NLM	0.64515	0.40236	0.30114	0.23787	0.20647	0.1796	0.16293	0.15868	0.15742
Anisotropic	0.72606	0.56728	0.44422	0.37154	0.30508	0.25325	0.20999	0.18127	0.15816
CNN	0.566137	0.404644	0.315003	0.271335	0.24121	0.220707	0.208054	0.198348	0.194117

4. Discussion

In the MRI imaging modality, the superposition of the linear magnetic field gradient on the uniform magnetic field applied to the patient is performed. When this superposition occurs, resonance frequencies of precessing nuclei depend primarily on the positions along the direction of the field gradient and produce a one-dimensional image. By taking the series of these projections along different gradient orientations, three-dimensional images are obtained. The value of the pixel of an image varies on the nature of the organs being scanned. The various performance metrics obtained by applying various filters to MRI uterus images aid in determining the filters' efficiency to remove various additive noises with an increasing percentage. The PSNR value obtained shows that the CNN proves to be better at filtering speckle and salt and pepper noises; whereas, NLM works efficiently in removing the Gaussian noise. The PSNR value obtained for different variances of the NLM filter for additive Gaussian noise of 10% was 14.52, 22.90, and 22.74, respectively [6]. Similarly, the SSIM metrics were evaluated better by CNN in filtering the speckle and salt and pepper noises, and the NLM filter efficiency for removing Gaussian noise was high comparatively. This proves that CNN performs better in maintaining the structural similarity by removing the speckle noise by obtaining a percentage of 92%.

From the various values obtained for the metrics, IQI shows that the bilateral filter was efficient in filtering Gaussian noise. Whereas, it was observed that both the bilateral and CNN filters were efficient enough in filtering the speckle noise, the anisotropic diffusion filter performed better in removing salt and pepper noise. The average time taken for the filtering process also provides outperforming results with the values for the Bilateral filter: 0.258 seconds, NLM filter: 0.834 seconds, anisotropic diffusion filter: 0.181 seconds, and CNN: 1.800 seconds. On taking a comparative analysis for time complexity, the CNN algorithm consumes more time than the anisotropic diffusion process.

5. Conclusion

The possibility of noise occurrence in the MR modality of imaging is increased due to various factors. Diagnosing the affected regions of tissues remains a challenging task

in the presence of noise pixels. Much research was performed to denoise the image to increase the quality of the MR image for further diagnostic procedures. These algorithms perform the denoising operation by which the efficiency of the filters is analyzed. In this paper, a comparative analysis of the denoising procedure using bilateral, NLM, anisotropic diffusion, and CNN filtering was performed. Performance metrics such as PSNR, SSIM, IQI, and time taken for the process were also calculated. This study proves that each filter performs and provides an outperforming result in different parameters.

References

- 1- Saime Akdemir Akar, "Determination of optimal parameters for bilateral filter in brain MR image denoising." *Applied soft computing*, Vol. 43, pp. 87-96, (2016).
- 2- Muhammad Sharif, Ayyaz Hussain, Muhammad Arfan Jaffar, and Tae-Sun Choi, "Fuzzy-based hybrid filter for Rician noise removal." *Signal, Image and Video Processing*, Vol. 10, pp. 215-24, (2016).
- 3- José V Manjón, Pierrick Coupé, and Antonio Buades, "MRI noise estimation and denoising using non-local PCA." *Medical image analysis*, Vol. 22 (No. 1), pp. 35-47, (2015).
- 4- Bin Liu, Xinzhu Sang, Shujun Xing, and Bo Wang, "Noise suppression in brain magnetic resonance imaging based on non-local means filter and fuzzy cluster." *Optik*, Vol. 126 (No. 21), pp. 2955-59, (2015).
- 5- Liu Chang, Gao ChaoBang, and Yu Xi, "A MRI denoising method based on 3D nonlocal means and multidimensional PCA." *Computational and mathematical methods in medicine*, Vol. 2015(2015).
- 6- Geng Chen, Bin Dong, Yong Zhang, Weili Lin, Dinggang Shen, and Pew-Thian Yap, "Denoising of diffusion MRI data via graph framelet matching in xq space." *IEEE Transactions on Medical Imaging*, Vol. 38 (No. 12), pp. 2838-48, (2019).
- 7- M Tabatabaeefar and A Mostaar, "Biomedical image denoising based on hybrid optimization algorithm and sequential filters." *Journal of biomedical physics & engineering*, Vol. 10 (No. 1), p. 83, (2020).
- 8- R Kala and P Deepa, "Adaptive fuzzy hexagonal bilateral filter for brain MRI denoising." *Multimedia Tools and Applications*, Vol. 79pp. 15513-30, (2020).
- 9- MHO Rashid, MA Mamun, MA Hossain, and MP Uddin, "Brain tumor detection using anisotropic filtering, SVM classifier and morphological operation from MR images." in *2018 international conference on computer*,

- communication, chemical, material and electronic engineering (IC4ME2)*, (2018): *IEEE*, pp. 1-4.
- 10- Prasun Chandra Tripathi and Soumen Bag, "CNN-DMRI: a convolutional neural network for denoising of magnetic resonance images." *Pattern Recognition Letters*, Vol. 135pp. 57-63, (2020).
- 11- Yuhan Zhang, Zhipeng Yang, Jinrong Hu, Shurong Zou, and Ying Fu, "MRI denoising using low rank prior and sparse gradient prior." *IEEE Access*, Vol. 7pp. 45858-65, (2019).